Gosha-jinki-Gan (GJG) shows anti-aging effects through suppression of TNF-α production by Chikusetsusaponin V

Keisuke Hagihara (hagihara.keisuke@gmail.com)
    Osaka University

Kazuto Nunomura
    Osaka University

Bangzhong Lin
    Osaka University

Megumi Fumimoto
    Osaka University

Junko Watanabe
    Tsumura Research Institute (Japan)

Yasuharu Mizuhara
    Tsumura Research Institute (Japan)

Research Article

Version of Record: A version of this preprint was published at Gene on January 1st, 2022. See the published version at https://doi.org/10.1016/j.gene.2021.146178.

Abstract

Frailty develops due to multiple factors, such as sarcopenia, chronic pain, and dementia. Go-sha-jinki-Gan (GJG) is a traditional Japanese herbal medicine used for age-related symptoms. We have reported that GJG improved sarcopenia, chronic pain, and central nervous system function through suppression of TNF-α production. In the present study, GJG was found to reduce the production of TNF-α in the soleus muscle of senescence-accelerated mice at 12 weeks and 36 weeks. GJG did not change the differentiation of C2C12 cells with 2% horse serum. GJG significantly decreased the expression of MAFbx induced by TNF-α in C2C12 cells on real-time PCR. TNF-α significantly decreased the expression of PGC-1α and negated the enhancing effect of GJG for the expression of PGC-1α on digital PCR. Examining 20 chemical compounds derived from GJG, cinnamaldehyde from cinnamon bark and Chikusetsusaponin V (CsV) from Achyrantes Root dose-dependently decreased the production of TNF-⬚ in RAW264.7 cells stimulated by LPS. CsV inhibited the nuclear translocation of NF-κB p65 in RAW264.7 cells. CsV showed low permeability using Caco-2 cells. However, the plasma concentration of CsV was detected from 30 minutes to 6 h and peaked at 1 h in the CD1 (ICR) mice after a single dose of GJG. In 8-week-old SAMP8 mice fed 4% (w/w) GJG from one week to four weeks, the plasma CsV concentration ranged from 0.0500 to 10.0 ng/mL. The evidence that CsV plays an important role in various anti-aging effects of GJG via suppression of TNF-⬚ expression is presented.

Introduction

Frailty is becoming one of the most important problems for clinical practice and public health in the world[1]. In particular, the population of elderly people in Japan is increasing more rapidly than that of any other country[2]. It is an urgent task to establish strategies against frailty to prevent an increase in the bedridden and nursing care population. First, the physical aspects of the frailty phenotype require attention. Fried et al reported that frailty is composed of weak grip strength, slow gait speed, low physical activity, exhaustion, and unintentional weight loss[3]. After various discussions, the concept of frailty has changed. Currently, frailty is thought to be multidimensional, involving both physical and psychosocial factors. As to the physical aspects of frailty, sarcopenia has been gaining attention. Sarcopenia denotes the decrease in muscle strength and muscle mass associated with aging[4]. Sarcopenia is thought to be caused by a variety of factors, such as aging-related decreases in physical activity, in addition to changes in nutrient intake, hormones, and the inflammatory response[5]. At least 50% of individuals ≥80 years old reportedly have sarcopenia[6]. Additionally, chronic pain control due to lumbago and arthralgia is important for maintaining continuity of rehabilitation and exercise to prevent sarcopenia. With respect to the psychosocial aspects of frailty, depression and dementia induce withdrawal and loneliness, resulting in the development of sarcopenia[1]. Given the multidimensional aspects of frailty, new pharmacotherapies need to be developed.

In traditional Japanese herbal medicine (Kampo medicine), Go-sha-jinki-gan (GJG) has been used to alleviate various types of age-related conditions, e.g. lumbago, numbness, and nocturia [7,8]. In Japan, it is

well known that GJG has a certain level of clinical effect for the above age-related symptoms. However, the pharmacological mechanism of GJG has yet to be elucidated in detail. Anticipating the anti-aging effect of GJG, the anti-sarcopenic effect of GJG was evaluated in senescence-accelerated mice (SAMP8), which are widely used in aging research[9]. We reported that GJG had a clear anti-sarcopenic effect on SAMP8 mice by improving the insulin-like growth factor (IGF-1) signaling pathway, increasing peroxisome proliferator-activated receptor-γ coactivator-1 alpha (PGC-1α) in the mitochondrial network, and decreasing the concentrations of tumor necrosis factor-alpha (TNF-α) in muscle[10]. Focusing on the decreased production of TNF-α, we examined the pain-relieving effect of GJG using chronic constriction injury (CCI) model mice. GJG significantly improved allodynia and hyperalgesia on the von Frey test, the cold-plate test, and the hot-plate test through suppression of TNF-α expression derived from activated microglia in the spinal cord of CCI model mice[11]. Next, we investigated whether GJG affects the central nervous system. GJG significantly prevented the paralytic symptoms in experimental allergic encephalomyelitis (EAE) model mice by decreasing TNF-α production derived from activated microglia in the brain[12].

Taken together, GJG improved sarcopenia, chronic pain, and central nervous system function through the suppression of TNF-α production from macrophage cells. However, it is unclear which botanical herbs or chemicals derived from GJG are mainly involved in decreasing TNF-α production. GJG consists of ten medicinal herbs in fixed proportions. Examining various chemical compounds derived from the component herbs of GJG, we found that Chikusetsusaponin V (CsV), which is derived from Achyranthes Root, dose-dependently decreased the production of TNF-α and the NF-κB signaling pathway. Moreover, we confirmed that CsV was detected in mice plasma after oral administration. In this study, the evidence that CsV plays an important role in the various effects of GJG through suppression of TNF-α expression is presented.

Results

GJG decreased the expression of TNF-α in the soleus muscle of SAMP8 mice at 12 and 36 weeks.

We previously reported the anti-sarcopenic effect of GJG in SAMP8 mice. GJG decreased the expression of TNF-α in the soleus muscle of SAMP8 mice at 38 weeks[10]. We found that GJG suppressed the production of TNF-α from activated microglia cells[11, 12]. We investigated the time-course of TNF-α and IL-6 expressions after GJG administration in SAMP8 and SAMR1 mice from 12 weeks to 48 weeks (Fig. 1a). No significant difference was observed in body weight and blood sugar regardless of GJG administration, the same as before the examination (data not shown). The soleus muscles were collected in SAMP8 and SAMR1 mice at 12, 16, 24, 36 and 48 weeks. Western blotting analysis showed that the expression of TNF-α in SAMP8 soleus muscles increased from 12 weeks to 36 weeks compared to that in SAMR1 mice and decreased with GJG administration at 12 weeks and 36 weeks (Fig. 1b,c). On the other hand, the expression of IL-6 in SAMP8 soleus muscle decreased slightly at 12 weeks, but was not changed from 16 weeks to 48 weeks, the same as in SAMR1 (Fig. 1d,e).

GJG decreased the expression of MAFbx in C2C12 cells after TNF-α stimulation

We previously reported that GJG improved the IGF-1 signaling pathway and increased PGC-1α in the soleus muscle of SAMP mice[10]. We examined whether GJG has a direct effect on muscle cells using mouse skeletal muscle cell line C2C12 cells. The C2C12 cells differentiated to myotube cells with DMEM containing 2% horse serum[13]. At the same time, they were treated with 10 μg/mL, 100 μg/mL, or no GJG. We expected that GJG would directly affect muscle atrophy, but GJG did not change the differentiation of C2C12 cells to myotubes with 2% horse serum (Fig. 2a). It is well known that MAFbx and MuRF-1 suppress the degradation of skeletal muscle protein[14,15]. We investigated the expression levels of MAFbx and MuRF1 using real-time RT-PCR 3 h after 10–100 ng/ml of TNF-α or no TNF-α; 10 ng/mL of TNF-α significantly induced the expression of MAFbx compared to non-stimulated cells (1.12 ± 0.047 vs 2.90 ± 0.10 fold changes, $P < 0.0001$ Tukey-Kramer test). GJG significantly decreased the expression of MAFbx induced by TNF-α from 2.90 ± 0.10 to 1.63 ± 0.003 fold changes ($P < 0.0001$ Tukey-Kramer test). The same results were obtained with stimulation by 100 ng/mL TNF-α (Fig. 2b). On the other hand, TNF-α stimulation did not change the expression of MuRF-1 with or without GJG (Fig. 2c). Next, the expression of PGC-1α with various stimuli was examined in C2C12 cells using real-time RT-PCR. GJG increased the expression of PGC-1α by less than 1.5 times, and TNF-α decreased the expression of PGC-1α by more than 0.5 (data not shown). In general, it is difficult to distinguish the expression of the target gene less than 2 times or more than half using real-time RT-PCR. Therefore, a digital RT-PCR assay was used to evaluate the expression of PGC-1α. GJG significantly increased the expression of PGC-1α from 0.980 ± 0.08 to 1.183 ± 0.10 fold changes ($P < 0.05$ Dunnett's test, Fig. 2d). TNF-α significantly decreased the expression of PGC-1α and negated the enhancing effect of GJG on the expression of PGC-1α. These results suggest that TNF-α plays a central role in the pathogenesis of sarcopenia. These results are consistent with the reports related to sarcopenia and inflammation, especially TNF-α [16–19]. We hypothesized that GJG shows an anti-sarcopenic effect through suppression of TNF production. Next, whether 20 chemicals derived from GJG and one control chemical derived from another botanical herb have an effect on TNF-α production was examined using RAW 264.7 cells, a mouse macrophage cell line.

GJG-derived chemicals decreased TNF-α expression by inhibition of nuclear translocation of NF-κB p65 in RAW 264.7 cells

GJG is composed of ten medicinal herbs in fixed proportions (Fig. 3a). It is well known that RAW 264.7 cells produce TNF-α with stimulation by lipopolysaccharide (LPS). We have previously reported that GJG prevented the production of TNF-α by RAW 264.7 cells stimulated with LPS in a dose-dependent manner[11]. On the other hand, GJG did not show a clear dose-dependent inhibitory effect of IL-6 in the same assay system (Fig. 1S). Thus, 20 chemical compounds derived from GJG and a negative control compound from another herbal medicine were selected based on analysis of the three-dimensional high-performance liquid chromatography profile and LC/MS analysis of GJG[10]. It was found that cinnamaldehyde from cinnamon bark and CsV from Achyrantes Root decreased the production of TNF-α from RAW 264.7 cells stimulated with LPS without cytotoxicity (Fig. 3b). It was confirmed that

cinnamaldehyde and CsV significantly inhibited the expression of TNF-α in a dose-dependent manner compared to control with DMSO (7064.1 ± 598.9 pg/mL vs 3792.4 ± 598.9 pg/mL, 3942.4 ± 598.9 pg/mL, P < 0.05 Tukey-Kramer test, Fig. 3c). Rokumi-Gan (RJG) consists of six medicinal herbs without cinnamon bark and Achyrantes Root (Fig. 3a), which means that RJG does not prevent the production of TNF-α. It was confirmed that RJG did not have an anti-sarcopenic effect in SAMP8 mice (Figure S2). These results suggest that cinnamaldehyde and CsV play important roles via the suppression of TNF-α levels. It is difficult to evaluate cinnamaldehyde in human blood because cinnamon bark is a common daily food. CsV is also detected from *Panax japonicus*, recognized as a very important medical herb[20,21]. Therefore, we focused on CsV as a drug efficacy marker of GJG.

Toll like receptor (TLR) 4 is well known as a receptor for LPS[22]. Therefore, whether GJG affected the expression of TLR4 signaling molecule was examined. GJG did not change the protein levels of TLR4 and MyD88 on Western blotting analysis (Fig. 4a). Next, whether GJG has an effect on the nuclear translocation of NF-κB p65 was examined, because NF-κB p65 is downstream of the TLR4 signaling pathway. In general, LPS stimulation activates the phosphorylation of IκBα Ser 32[23]. As a result, IκBα is degraded via ubiquitination, and NF-κB p65 translocates to the nucleus[23]. The same results were observed in the present study, and GJG inhibited the phosphorylation of IκBα Ser 32 and nuclear translocation of NF-κB p65 in a dose-dependent manner (Fig. 4b). In almost the same manner, CsV showed nuclear translocation of NF-κB p65 in a dose-dependent manner (Fig. 4c). These results indicated that CsV has an anti-inflammatory effect on RAW 264.7 cells through its inhibitory effect on nuclear translocation of NF-κB p65. These results suggest that CsV is a pharmacological marker for the anti-inflammatory effect of GJG. Then, the characteristics of CsV as a drug compound were investigated.

CsV showed high solubility, low permeability, and high metabolic stability

CsV has a saponin structure, as shown in Fig. 5a. Saponin has multiple hydrophilic sugars bound to a hydrophobic skeleton. To examine the solubility of CsV with PBS, the supernatant of 1% or 5% DMSO/PBS solution of CsV was examined using an LC/MS assay system, and the solubility was calculated based on the area under the curve (AUC). Figure 5b shows the single peak of the supernatant of 5% DMSO/PBS solution of CsV; 500 μM of CsV with 5% DMSO showed an AUC about 10 times greater than that of 50 μM of CsV with 5% DMSO, and 500 μM of CsV with 1% DMSO showed almost the same AUC as that of 500 μM of CsV with 5% DMSO (Fig. 5c). These results show that CsV has more than 95% solubility with PBS.

Next, the membrane permeability of CsV was examined, because herbal medicine is generally given orally. The caco-2 permeability assay system[24] was used, and the permeability coefficient (Papp) of CsV was calculated. The Papp of CsV was less than 0.1 cm/sec x 10^{-6}, which indicates that CsV has very low membrane permeability (Fig. 5d). Metabolic stability is said to be important to maintain blood concentrations of chemical compounds. To examine the metabolic stability of CsV, CsV was mixed with liver microsomes, coenzyme group (NADPH, G-6-P) and G6PDH, at 37 °C for 10 min and 60 min. Unchanged CsV compounds were detected at above 80% at 10 and 60 min compared to the unchanged

CsV before treatment as 100% (Fig. 5e). These results show that CsV has high metabolic stability. Next, whether Csv can be detected in the plasma of mice following oral administration of GJG was examined, because the permeability of CsV is very low.

CsV was detected in the plasma of CD1 (ICR) mice and SAMP8 mice following oral administration of GJG

A single dose of GJG 1 g/kg was given to 8-week-old CD1 (ICR) mice fasted for 16 h, and changes in plasma CsV levels were examined. An LC-MS/MS assay system detecting a single peak of CsV in CD1 (ICR) mice plasma from 0.0200 to 10.0 ng/mL was established (Fig. 6a,b). After a single dose of GJG, the plasma concentration of CsV was detected from 30 min to 6 h and peaked at 1 h (Fig. 6c).

Finally, changes of plasma levels of CsV were examined in 8-week-old SAMP8 mice fed a normal diet or a normal diet supplemented with 4% (w/w) GJG from one week to four weeks. In SAMP8 mice, the plasma concentration of CsV ranged from 0.0500 to 10.0 ng/mL. Although there were variations depending on the individual mice, CsV was clearly detected in the plasma of SAMP8 mice fed a GJG-containing diet from one week to four weeks. On the other hand, CsV was not detected in mice fed a normal diet. These results clearly showed that CsV is absorbed into blood following oral administration of GJG and plays a central role in the anti-inflammatory effect of GJG.

Discussion

In this study, GJG was shown to inhibit TNF-α production in vivo and in vitro. Investigating the inhibitory mechanism of GJG using various chemical compounds, it was found that CsV derived from Achyranthes Root, a component of GJG, inhibited the nuclear translocation of NF-kB p65 after LPS stimulation in RAW264.7 cells. In addition, CsV was detected following oral administration of GJG in the plasma of ICR (ICR) mice or SAMP8 mice. Therefore, these results show that CsV plays a pivotal role in the pharmacological effects of GJG on muscle, spinal cord, and brain.

We previously reported that GJG improved the amounts of skeletal muscles fibers and fiber types in SAMP8 mice at 38 weeks[10]. We expected that GJG would have a direct effect on muscle atrophy, but GJG did not change the differentiation of mouse skeletal muscle cell line C2C12 cells to myotubes using 2% horse serum. These results suggest that GJG did not have a direct effect on C2C12 cells. Higher serum levels of TNF-α were reported in elderly people with sarcopenia compared to healthy controls[16–18]. It has been reported that TNF-α induces muscle atrophy in aged mice and TNF transgenic mice[19]. Thus, these reports suggest that TNF-α is required in the pathogenesis of sarcopenia. To examine the effect of GJG on C2C12 cells, TNF-α stimulation was added in the supernatant of the culture medium. It was found that GJG inhibited the expression of MAFbx induced by TNF-α at 3 h in C2C12 cells. MAFbx has been reported to be expressed by TNF-α via p38 in C2C12 cells from 2 h to 4 h[25]. These results were consistent with the present results. On the other hand, MuRF-1 was not induced by TNF-α in the present assay system using C2C12 cells. It has been reported that MuRF-1 was induced by TNF-α at 24 h after stimulation [26]. In the

present study, the expression of MuRF-1 was evaluated 3 h after TNF-α stimulation. One of the reasons for the different results is that the expression of MuRF-1 was evaluated at a different time after TNF-α stimulation. We have previously reported that administration of GJG increased serum levels of IGF-1 in SAMP8 mice at 38 weeks. IGF-1 is required for skeletal muscle hypertrophy[14, 15]. Plasma IGF-1 concentrations decrease with aging[27]. In an aging mice assay, the insulin/IGF-1 signaling pathway also regulates the expression of MuRF-1. With an in vitro assay using C2C12 cells, IGF-1 was not used in the supernatant of the culture medium, which might cause different experimental results.

We previously reported that GJG increased the protein level of PGC-1α in SAMP8 mice at 38 weeks. PGC-1α is known to be one of the main regulators of mitochondrial biogenesis and regulates muscle fiber types[28, 29]. It has been reported that mitochondrial fission causes muscle atrophy[30]. We examined whether GJG directly increases PGC-1α using a real-time PCR assay system, but the results were controversial because GLG changed the expression of PGC-1α slightly. Since mitochondrial DNA levels in peripheral blood mononuclear cells decrease gradually with aging, it is difficult to quantify mitochondrial genes using real-time PCR. Real-time PCR is less sensitive because it calculates the mitochondrial DNA copies compared to a housekeeping gene [31]. Digital PCR has been used in clinical microbiology, for example HIV, because it allows for absolute target measurement by directly counting single droplets[32,33]. Digital PCR has been shown to be useful for measuring mitochondrial genes[31]. We showed that GJG increased the expression of PGC-1α slightly, but significantly, using a digital PCR assay system. TNF-α suppressed the expression of PGC-1α and negated the increasing effect of GJG. It has been reported that TNF-α decreased the mRNA of PGC-1α in C2C12 myotube cells[34, 35]. The present results and former reports indicate that it is important to regulate the expression levels of TNF-α, which affects the mitochondrial function of muscle.

As a method of searching for active ingredients of herbal medicines, separation of a solution of a herbal medicine into fractions is performed, and the effects of each fraction are examined. The chemical compounds of GJG have been previously identified based on the three-dimensional high-performance liquid chromatography profile and LC/MS analysis against GJG[10]. Although it is necessary to know the ingredients to some extent, the advantages of our methods are that they can examine the dose dependency of chemical compounds and confirm the reproducibility of experimental results. Two active compounds were detected from GJG, cinnamaldehyde and CsV. It has been reported that cinnamaldehyde inhibited the production of TNF-α stimulated by LPS in RAW 264.7 cells[36]. The present results do not contradict previous reports. Cinnamon bark is one of the components of Kakkon-to, a traditional herbal medicine, which has been used for the treatment of influenza and the common cold[37]. CsV is noted as one of the active components of *Panax japonicus*, the most famous herbal medicine because of its anti-aging effect. Total saponin of *Panax japonicus* contains Cs II, IV, IVa, and V[21]. It has been reported that CsV and CsIVa have anti-inflammatory effects by inhibiting the NF-κB signaling pathway in RAW 264.7 cells stimulated by LPS[21]. The present results and previous reports show that cinnamaldehyde and CsV prevent TNF-α production by macrophage cells stimulated with LPS. In fact, RJG, composed of six traditional herbs without cinnamon bark and Achyrantes Root, did not have an anti-

sarcopenic effect in SAMP8 mice. These results suggest that cinnamaldehyde and CsV might be biomarkers of the pharmacological effect of GJG. However, cinnamon bark is commonly used as a food ingredient and might be detected in the plasma without administration of GJG. On the other hand, Achyrantes Root is only used as a herbal medicine. Therefore, we focused our attention on CsV, one of the main active compounds of Achyrantes Root. The characteristics of CsV as a chemical compound remain unknown. We established a CsV detection system with LC-MS and showed that CsV has low permeability and high metabolic stability. As far as we know, this is the first report of the characteristics of the chemical compound of CsV. Based on permeability experiments, low absorption of CsV following oral administration is expected. However, CsV was clearly detected in the plasma of CD1 (ICR) mice with single administration and SAMP8 mice with continuous administration. It has been reported that herbal medicines are quickly absorbed by transporters[38]. Therefore, unknown transporters are likely involved in the absorption of CsV. Further study is needed to clarify the precise mechanism of CsV absorption.

Thus, this study demonstrated that GJG inhibited the production of TNF-α in the soleus muscle of SAMP8 mice biphasically. GJG directly inhibited the expression of TNF-α from RAW 264.7 cells via the derived compounds, cinnamaldehyde and CsV. CsV was clearly detected in the plasma of SAMP8 mice following oral administration of GJG. These results suggest that CsV is a promising candidate for monitoring the pharmacological effects of GJG.

Materials And Methods

Preparation of GJG extract and chemical compounds

GJG extract powder was purchased from Tsumura & Co. (Tokyo, Japan). GJG extract powder was suspended in Dulbecco's modified Eagle's medium (DMEM) (Wako, Osaka, Japan) and autoclaved (121°C, 15 min). After autoclaving, fetal bovine serum (FBS) (Sigma, Marlborough, MA, USA) was added so that the final concentration was 10%, and the mixture was passed through a 0.22-μm filter. Chemical compounds were selected and purchased based on the three-dimensional high-performance liquid chromatography profile and LC/MS analysis of GJG[10] as below: benzoylpaeoniflorin (Cheminstock Ltd., Shanghai, China), Paeoniflorin, Genipin, 2'-hydroxy-4'-methyoxyacetophenone, morroniside, cinnamaldehyde (AK Scientific, Inc., Union City, CA, USA), Loganin, Isoacteoside (BioBioPha Co., Ltd., Kunming, China), Geniposidic acid, Benzoylmesaconine, Chikusetsusaponin V, Mesaconitine, Catalpol, Alisol A, Neoline, Benzoylaconine, Aucubin (Chemexpress Co., Ltd., Shanghai, China), Benzoylhypaconine (JR MediChem LLC, Princeton, NJ, USA), Azomycin (Selleck Chemical, Houston, TX, USA), 1,2,3,4,6-penta-O-galloyl-β-D-glucopyranose (Toronto Research Chemicals, Toronto, Canada), and Inokosterone (ChemFaces Biochemical Co., Ltd., Wuhan, China).

Animals

SAMP8 and SAMR1 mice (8 weeks old), purchased from SLC, Inc. (Shizuoka, Japan), were divided into two groups of 5 each one week after they were acclimated based on the diet that they were fed: a normal diet (powdered mouse food; Oriental Yeast Co. Ltd. (Tokyo, Japan; P8 + N group); and a normal diet

supplemented with 4% (w/w) GJG (P8 + GJG group). The control group, which consisted of 8-week-old male SAMR1 mice also purchased from SLCm was also divided into two groups of 10 each based on the diet that they were fed: a normal diet (R + N group); and a normal diet supplemented with 4% (w/w) GJG (R + GJG group). The general conditions and body weight of all mice were recorded. Housing care and the experimental protocol were performed according to the National Institutes of Health Guide for the Care and Use of Laboratory Animals and with the approval of the Animal Care and Use Committee of Osaka University. We confirmed the study was carried out in compliance with the ARRIVE guidelines

Cell Culture And Immunofluorescence Staining

Mouse skeletal muscle cell line C2C12 cells were obtained from DS Pharma Biomedical (Osaka, Japan). C2C12 cells were seeded in a 6-well plate at 5×10^4 cells/ml and cultured in DMEM containing 10% FBS, 100 U/mL penicillin, and 100 ug/mL streptomycin (Nacalai, Kyoto, Japan) for 48 h. After 100% confluence, the medium was replaced with DMEM containing 2% horse serum (Gibco BRL, Grand Island, NY, USA) and cultured for 96 h. Differentiation of C2C12 cells from myoblasts to myotubes was confirmed using immunofluorescence staining of sarcomeric α actinin[13]. C2C12 cells were fixed with 4% paraformaldehyde solution in PBS at room temperature for 10 min and permeabilized with 1 mL of 0.25% Triton/PBS for 20 min. After blocking with 5% skim milk/PBS at room temperature for 30 min, anti-Sarcomeric Alpha Actinin antibody (ab9465) (Abcam, Cambridge, UK) with 5% skim milk/PBS was added to the dilution and left overnight at 4°C. The secondary antibody was diluted with PBS, the diluted solution was added, shielded from light with aluminum foil, and allowed to stand at room temperature for 1 h. Nuclear staining was performed with DAPI-containing encapsulant (ProLong ™ Gold Antifade Mountant with DAPI: Invitrogen) on a glass slide[13].

Real-time Quantitative PCR And Droplet Digital PCR

The differentiated C2C12 myotubes underwent treatment with 100 μg/mL GJG, and then, 24 h later, the medium was replaced with a serum-free DMEM medium containing 100 μg/mL GJG and 10 or 100 ng/mL murine TNF-α (Peprotech, Rocky Hill, NJ). Then, 0, 3, and 6 h after the medium was changed, total RNA was extracted using the RNeasy Mini Kit (Qiagen, Valencia, CA) according to the manufacturer's instructions. Subsequently, SuperScript VILO Master Mix (Invitrogen, Carlsbad, CA) was used to synthesize cDNA from 200 ng of RNA. The ViiA 7 real-time PCR system (Life Technologies, Carlsbad, CA, USA) was used for real-time quantitative PCR, with the following cycling conditions: 50 ºC for 2 min, 95 ºC for 20 sec, followed by 40 cycles of 95 ºC for 1 sec and 60 ºC for 20 sec at annealing temperature. TaqMan Fast Advanced master mix (Applied Biosystems, Foster City, CA) was used to amplify the target genes from 10 ng of cDNA. Gene-specific primers and FAM-labeled probes (mouse MAFbx: Mm00499523_m1, mouse MuRF1: Mm01185221_m1, mouse PGC1-α: Mm01208835_m1, mouse B2M: Mm00437762_m1) were purchased from Applied Biosystems. Relative expression levels relative to beta2 macroglobulin (B2M) expression were then calculated.

A QX100 droplet digital PCR (ddPCR) system (Bio-Rad Laboratories, Hercules, CA) was used for ddPCR in a total volume of 20 µL, with 10 µL 2x ddPCR Supermix for the probes (Bio-Rad Laboratories), 1 µL primers and FAM-labeled probes (mouse B2M: Mm00437762_m1, mouse PGC1-α: Mm01208835_m1), and 5 µL sample cDNA (10 ng total RNA). After droplets were generated with a QX100 Droplet Generator (Bio-Rad Laboratories), a C1000 Touch Thermal Cycler (Bio-Rad Laboratories) was used to amplify each cDNA. The thermal cycling conditions were as follows: a pre-cycling hold at 95 ºC for 10 min, followed by 40 cycles of 94 ºC for 30 sec and 58 ºC for 1 min, with final heating at 98 ºC for 10 min. A QX100 Droplet Reader (Bio-Rad Laboratories) was used to measure droplets, and QuantaSoft software version 1.6.6 (Bio-Rad Laboratories) was used to analyze the target copy number, with normalization of the target copy number by B2M.

TNF-α ELISA and cell viability assay

A mouse macrophage cell line (RAW264.7), purchased from Dainippon Pharmaceutical (Osaka, Japan), was grown in DMEM with 10% FBS, 100 µg/mL streptomycin, and 100 U/mL penicillin at 37°C in a humidified 5% CO_2 atmosphere. LPS was purchased from Sigma-Aldrich (St. Louis, MO, USA). The RAW264.7 cells were seeded in triplicate at 5×10^4 cells/mL in 96-well plates and left for 48 h. At that point, the cells were cultured for 24 h in DMEM with or without 10 or 100 µg/mL GJG (final 1% FBS). This was followed by stimulation of the cells by 10 ng/mL LPS for 16 h. The TNF-α concentration in the supernatant of the medium was then evaluated with a mouse TNF-α Quantikine ELISA kit (R & D Systems, Minneapolis, MN, USA) according to the manufacturer's instructions [11]. Cell viability, evaluated using Cell Counting kit-8 (Dojindo, Kumamoto, Japan) according to the manufacturer's protocol, was calculated by comparison to that of cells without GJG and LPS. Each of the above experiments was performed at least three times, and representative data are reported.

Western Blotting Analysis

SAMP8 and SAMR1 mice were sacrificed at 12, 16, 24, 36, and 48 weeks (each group, n = 3), and soleus muscles were obtained, with the muscle samples cut into small pieces and homogenized in RIPA buffer (Nacalai) with phosphatase inhibitor cocktail (Nacalai) and protease inhibitor cocktail (Thermo Fisher Scientific, Tokyo, Japan). After the lysates were centrifuged for 10 min at 14,000 g and 4°C, the supernatants were collected. The BCA Protein Assay Kit (Sigma) was then used to measure protein, followed by Western blot analysis according to previously described methods[10,11].

After seeding of RAW264.7 cells in triplicate at 1×10^5 cells/mL in 6-well plates, they were grown in DMEM with 10% FBS, 100 µg/mL streptomycin, and 100 U/mL penicillin at 37°C in a humidified 5% CO_2 atmosphere. Then, 48 h later, the cells were cultured for 24 h in DMEM with or without 10 or 100 µg/mL GJG (final 1% FBS). Dexamethasone(Dex) (Sigma, St Louis, MO, USA) was added for 24 h at 10−100 µM. To detect MyD88 and TLR4, cell stimulation was performed with 10 ng/mL LPS for 24 h, followed by homogenization of whole cell lysate in RIPA buffer with phosphatase inhibitor cocktail and protease inhibitor cocktail. To detect NF-κB p65, p-IκBα, and Ser32 IκBα, cell stimulation with 10 ng/mL LPS was performed for 30 min, followed by separation of nuclear extracts using NE-PER Nuclear and Cytoplasmic

Extraction Reagents (Thermo Fisher Scientific). The method described above was then used for Western blot analysis. Specific primary antibodies were then used for the following: TNF-α (Cell Signaling Technology #3707, Danvers, MA, USA); IL-6 (Cell Signaling Technology #3707); MyD88 (CST #4283); TLR4 (Santa Cruz Biotechnology sc-293072, Santa Cruz, CA, USA); IκBα (CST #9242); p-IκBα Ser32 (CST #2859); NF-κB p65 (CST #8242);GAPDH (CST); and PCNA (CST #13110).

Chemical Characteristic Analysis Of Chikusetsusaponin V

The solubility, membrane permeability, and metabolic stability of Chikusetsusaponin V were investigated. A 1% DMSO / PBS solution of Chikusetsusaponin V (final 500 μM) was created and filtered with a filtration plate (Multi Screen HTS-PCF, Merck-Millipore). Acetonitrile was added to the filtered samples, which were vortexed and centrifuged at 3500 rpm for 10 min. Supernatant was analyzed by LC/MS (Xevo TQ-S MS/MS, Milford, MA, USA). Solubility was calculated based on the area under the curve compared to 5% DMSO/PBS solution of Chikusetsusaponin V (final 50 μM or 500 μM). A caco-2 permeability assay was performed according to established methods[24].

Briefly, 500 μM Chikusetsusaponin V/HBSS solution was added to the upper wells of cultured Caco-2 cells in a trans-well-plate, and HBSS with 1% BSA was added to the lower wells. After incubation for 2 h, the solution on the top plate and the bottom plate was collected. Acetonitrile was added to the solution, which was vortexed and centrifuged at 3500 rpm for 20 min. The supernatant was analyzed by LC/MS (Xevo TQ-S), and the apparent permeability coefficient (Papp) was calculated. For the metabolic stability assay, 500 μM Chikusetsusaponin V was mixed with liver microsomes (Sekisui XenoTech, LLC, Kansas City, KS, USA, final concentration 0.2 mg protein/mL), coenzyme group (NADPH, G-6-P : Sigma, Marlborough, MA, USA, MgCl2 : Wako, Osaka, Japan), and G6PDH (Oriental Yeast, Tokyo, Japan) Mix (200 μL) at 37 ˚C, for 0 min, 10 min, and 60 min. Acetonitrile was added to the solution, which was vortexed and centrifuged at 3500 rpm for 20 min. The supernatant was analyzed by LC/MS (Xevo TQ-S), and the ratio of unchanged chemical compound at 10 min and 60 min compared to the unchanged Chikusetsusaponin V at 0 min as 100% was calculated.

Plasma assay of Chikusetsusaponin V in mice administered GJG orally

After fasting for 16 h, extract powder of GJG 1 g/kg was administered orally to 8-week-old male CD1 (ICR) mice (Charles River Laboratories Japan, INC., Kanagawa, Japan). Plasma samples were collected from the caudal vena cava (heparin treatment) before and after administration at 0.5, 1, 2, 4, 6, 8, 10, 12, and 24 h (n = 5 at each time point).

Eight-week-old, male SAMP8 mice were fed a normal diet (n = 3 from 1 week to 3 weeks, n = 6 at 4 weeks) or a normal diet supplemented with 4% (w/w) GJG for four weeks (n = 6 before and at each time point). Plasma samples were collected before and after administration at 1, 2, 3, and 4 weeks. Acetonitrile was added to the plasma samples, and the supernatants were collected after centrifugation. The supernatant was dried and dissolved in 100 μL of solution (10 mmol/L ammonium formate solution/acetonitrile (80:20)). The concentration of chikusetsusaponin V was measured by LC-MS / MS (MS / MS: QTRAP

5500; AB Sciex, Framingham, MA, HPLC: Agilent 1260; Agilent Technologies, Santa Clara, CA). The plasma concentration was calculated by adding a standard solution of chikusetsusaponin V (PhytoLab GmbH & Co. KG, Vestenbergsgreuth, Germany) to plasma to prepare a calibration curve. For analysis of CD1(ICR) mice analysis, the range of the calibration curve was from 0.0200 to 10.0 ng/mL and for SAMP8 mice, the range of the calibration curve was from 0.0500 to 10.0 ng / mL.

Statistical analysis

The real-time PCR results and the TNF-α ELISA results were analyzed using Tukey-Kramer's post hoc test, and the results of droplet digital PCR were examined by Dunnet's test using JAMP Pro version 14. A p-value less than 0.05 was considered significant.

Declarations

Acknowledgements

Author contributions statement

K.H. conceived and conducted all experiments. K.N., B.L., and M.F. analyzed in vitro data of Chikusetusaponin V. J.W. and Y.M. analyzed in vivo data of Chikusetusaponin V. All authors reviewed the manuscript.

Conflicts of Interest: Dr. Hagihara holds the position of Joint Research Chair in collaboration with Tsumura Co. who produced GJG. Watanabe and Mizushima are members of Tsumura Co. Other authors have no competing interests.

Additional information

Supplementary information is available for this paper.

**Correspondence** and requests for materials should be addressed to K.H.

References

1. 1 Hoogendijk, E.O., Afilalo, J., Ensrud, K.E., Kowal, P., Onder, G., Fried, L. P. Frailty: implications for clinical practice and public health. Lancet. **394**, 1365-1375 (2019).

2. Kojima, G., Steve Iliffe, S., Taniguchi, Y., Shimada, H., Rakugi, H, Walters, K. Prevalence of frailty in Japan: A systematic review and meta-analysis. J Epidemiol. **27**, 347-353 (2017).

3. Fried, L. P., Tangen, C. M., Walston, J., Newman, A. B., Hirsch, C., Gottdiener, J., et al. Frailty in older adults: evidence for a phenotype. J Gerontol A Biol Sci Med Sci.;**56**, M146-56 (2001).

4. Cruz-Jentoft A. J., Bahat, G., Bauer, J., Boirie, Y., Bruyère, O., Cederholm,T., et al. Sarcopenia: revised European consensus on definition and diagnosis. Age Ageing. **48**, 16-31(2019).

5. Ali, S., Garcia, J. M. Sarcopenia, cachexia and aging: diagnosis, mechanisms and therapeutic options - a mini-review. Gerontology **60**, 294-305 (2014).

6. Colón, C. J. P., Molina-Vicenty, I. L., Frontera-Rodríguez, M., García-Ferré, A., Rivera, B. P., Cintrón-Vélez, G., et al. Muscle and Bone Mass Loss in the Elderly Population: Advances in diagnosis and treatment. J Biomed (Syd). **3**, 40-49 (2018).

7. Hagihara, K., Yakubo, S., Namiki, T. Abbreviation of kampo formulations and basic terminology in kampo medicine. Traditional & Kampo Medicine. **4,** 65-88 (2017).

8. Usuki, Y., Usuki, S., Hommura, S. Successful treatment of a senile diabetic woman with cataract with goshajinkigan. Am J Chin Med **19**, 259-263 (1991)

9. Takeda, T., Matsushita, T., Kurozumi, M., Takemura, K., Higuchi, K., Hosokawa, M. Pathobiology of the senescence-accelerated mouse (SAM). Exp Gerontol. **32**, 117-127 (1997).

10. Kishida, Y., Kagawa, S., Arimitsua, J., Nakanishi, M., Sakashita, N., Shizue Otsuka, S., et al. Go-sha-jinki-Gan (GJG), a traditional Japanese herbal medicine, protects against sarcopenia in senescence-accelerated mice. Phytomedicine. **22**, 16-22 (2015).

11. Nakanishi, M., Nakae, A., Kishida, Y., Baba, K., Sakashita, N., Shibata, M., et al. Go-sha-jinki-Gan (GJG) ameliorates allodynia in chronic constriction injury-model mice via suppression of TNF-α expression in the spinal cord. Mol Pain. **12**: 10.1177/1744806916656382 (2016).

12. Jiang, S., Baba, K., Okuno, T., Kinoshita. M., Choong, C. J., Hayakawa, H., et al. Go-sha-jinki-Gan Alleviates Inflammation in Neurological Disorders via p38-TNF Signaling in the Central Nervous System. Neurotherapeutics. **20**, 10.1007/s13311-020-00948-w (2020).

13. Tanaka, Y., Kita, S., Nishizawa, H., Fukuda, S., Fujishima, Y., Obata, Y., et al. diponectin promotes muscle regeneration through binding to T-cadherin. Sci Rep. **9**,10.1038/s41598-018-37115-3 (2019).

14. Brunet, A., Bonni, A., Zigmond, M.J., Lin, M.Z., Juo, P., Hu, L.S., et al. Akt promotes cell survival by phosphorylating and inhibiting a Forkhead transcription factor. Cell. **96**, 857-868 (1999).

15. Franke, T.F., Kaplan, D. R., Cantley, L. C. PI3K: downstream AKTion blocks apoptosis. Cell. **88**, 435-437 (1997).

16. Brzeszczyńska, J., Meyer, A., McGregor, R., Schilb, A., Degen, S., Tadini, V. et al. Alterations in the in vitro and in vivo regulation of muscle regeneration in healthy ageing and the influence of sarcopenia. J Cachexia Sarcopenia Muscle. **9**, 93-105 (2018).

17. Li, C. W., Yu, K., Shyh-Chang, N., Li, G., X., Jiang, L. J., Yu, S. L., et al. Circulating factors associated with sarcopenia during ageing and after intensive lifestyle intervention. J Cachexia Sarcopenia

Muscle. **10**, 586-600 (2019).

18. Bian, A. L., Hu, H. Y., Rong, Y. D., Wang, J., Wang, J. X., Zhou, X. Z. A study on relationship between elderly sarcopenia and inflammatory factors IL-6 and TNF-alpha. Eur J Med Res. **22**, 10.1186/s40001-017-0266-9 (2017).

19. Li, J., Yi, X., Yao, Z., Chakkalakal, J. V., Xing, L., Boyce, B. F. TNF Receptor-Associated Factor 6 Mediates TNFalpha-Induced Skeletal Muscle Atrophy in Mice During Aging. J Bone Miner Res. **35**, 1535-1548 (2020).

20. Yuan, Q., Zhang, D., Liu, C., Zhang, C., Yuan, D. Chikusetsusaponin V Inhibits LPS-Activated Inflammatory Responses via SIRT1/NF-kappaB Signaling Pathway in RAW264.7 Cells. Inflammation. **41**, 2149-2159 (2018).

21. Xin, Y., Yuan, Q., Liu, C., Zhang, C., Yuan, D. MiR-155/GSK-3beta mediates anti-inflammatory effect of Chikusetsusaponin IVa by inhibiting NF-kappaB signaling pathway in LPS-induced RAW264.7 cell. Sci Rep. **10**: 10.1038/s41598-020-75358-1 (2020).

22. Takeda, K., Akira, S. Toll-like receptors in innate immunity. Int Immunol **17**, 1-14 (2005).

23. Karin, M., Ben-Neriah, Y. Phosphorylation meets ubiquitination: the control of NF-[kappa] B activity. Annu Rev Immunol. **18,** 621-663 (2000).

24. Matsumoto, T., Kaifuchi, N., Mizuhara, Y., Warabi, E., Watanabe, J. Use of a Caco-2 permeability assay to evaluate the effects of several Kampo medicines on the drug transporter P-glycoprotein. J Nat Med. **72,** 897-904 (2018).

25. Li, Y. P, Chen, Y., John, J., Moylan, J., Jin, B., Mann, D., L., et al. TNF-alpha acts via p38 MAPK to stimulate expression of the ubiquitin ligase atrogin1/MAFbx in skeletal muscle. FASEB J. **19**, 362-70 (2005).

26. Wang, D. T., Yin, Y., Yang, Y., J., Lv, P., J., Shi, Y., Lu, L., et al. Resveratrol prevents TNF-α-induced muscle atrophy via regulation of Akt/mTOR/FoxO1 signaling in C2C12 myotubes. International Immunopharmacology. **19**, 206-213 (2014).

27. Donahue, L., R., Hunter, S., J., Sherblom, A., P, Rosen, C. Age-related changes in serum insulin-like growth factor-binding proteins in women. J Clin Endocrinol Metab. **71,** 575-579 (1990).

28. Miura, S., Kai, Y., Ono, M., Ezaki, O. Overexpression of Peroxisome Proliferator-activated Receptor γ Coactivator-1α Down-regulates GLUT4 mRNA in Skeletal Muscles. J Biol Chem. **278**, 31385-31390 (2003).

29. Lin, J., Wu, H., Tarr, P. T., Zhang, C. Y., Wu, Z., Boss, O., Michael, L. F., et al. Transcriptional co-activator PGC-1 alpha drives the formation of slow-twitch muscle fibres. Nature. **418, 7**97-801 (2002).

30. Romanello, V., Guadagnin, E., Gomes, L., Roder, I., Sandri, C., Petersen, Y., et al. Mitochondrial fission and remodelling contributes to muscle atrophy. EMBO J. **29**, 1774-1785 (2010).

31. O'Hara, R., Tedone, E., Ludlow, A., Huang, E., Arosio, B., Mari,D., et al. Quantitative mitochondrial DNA copy number determination using droplet digital PCR with single-cell resolution. Genome Research. **29,** 1878-1888 (2019).

32. Rutsaert, S., Bosman, K., Trypsteen, W., Nijhuis, M., Vandekerckhove, L. Digital PCR as a tool to measure HIV persistence. Retrovirology. 16. 10.1186/s12977-018-0399-0 (2018).

33. Kuypers J., Jerom, K., R. Applications of Digital PCR for Clinical Microbiology.J Clin Microbiol. **55,** 1621-1628 (2017).

34. Remels, A. H., Gosker, H. R., Bakker, J., Guttridge, D. C., Schols, A. M., Langen, R. C. Regulation of skeletal muscle oxidative phenotype by classical NF-κB signalling. Biochim Biophys Acta. **1832,** 1313-1325 (2013).

35. Marzetti, E., Calvani, R., Cesari, M., Buford, T. W., Lorenzi, M., Behnke, B. J., et al. Mitochondrial dysfunction and sarcopenia of aging: from signaling pathways to clinical trials. Int J Biochem Cell Biol. **45,** 2288-2301 (2013).

36. Gunawardena, D., Karunaweera, N., Lee, S., Kooy, F. V. D., Harman, D. G., Raju, R., et al. Anti-inflammatory activity of cinnamon (C. zeylanicum and C. cassia) extracts - identification of E-cinnamaldehyde and o-methoxy cinnamaldehyde as the most potent bioactive compounds. Food Funct. **6**, 910-919 (2015).

37. Ishijima, Y., Kawamura, T., Kimura, A., Kohno, A., Okada. T., Tsuji, T., et al. Toll-like receptor 4-dependent adjuvant activity of Kakkon-to extract exists in the high molecular weight polysaccharide fraction. Int J Immunopathol Pharmacol. **24**, 43-54 (2011).

38. Ishiuchi, K., Morinaga, O., Ohkita, T., Tian, C., Hirasawa, A., Mitamura, M., et al. 18β-glycyrrhetyl-3-O-sulfate would be a causative agent of licorice-induced pseudoaldosteronism. Sci Rep. **9**, 1587. 10.1038/s41598-018-38182-2 (2019).

Figures
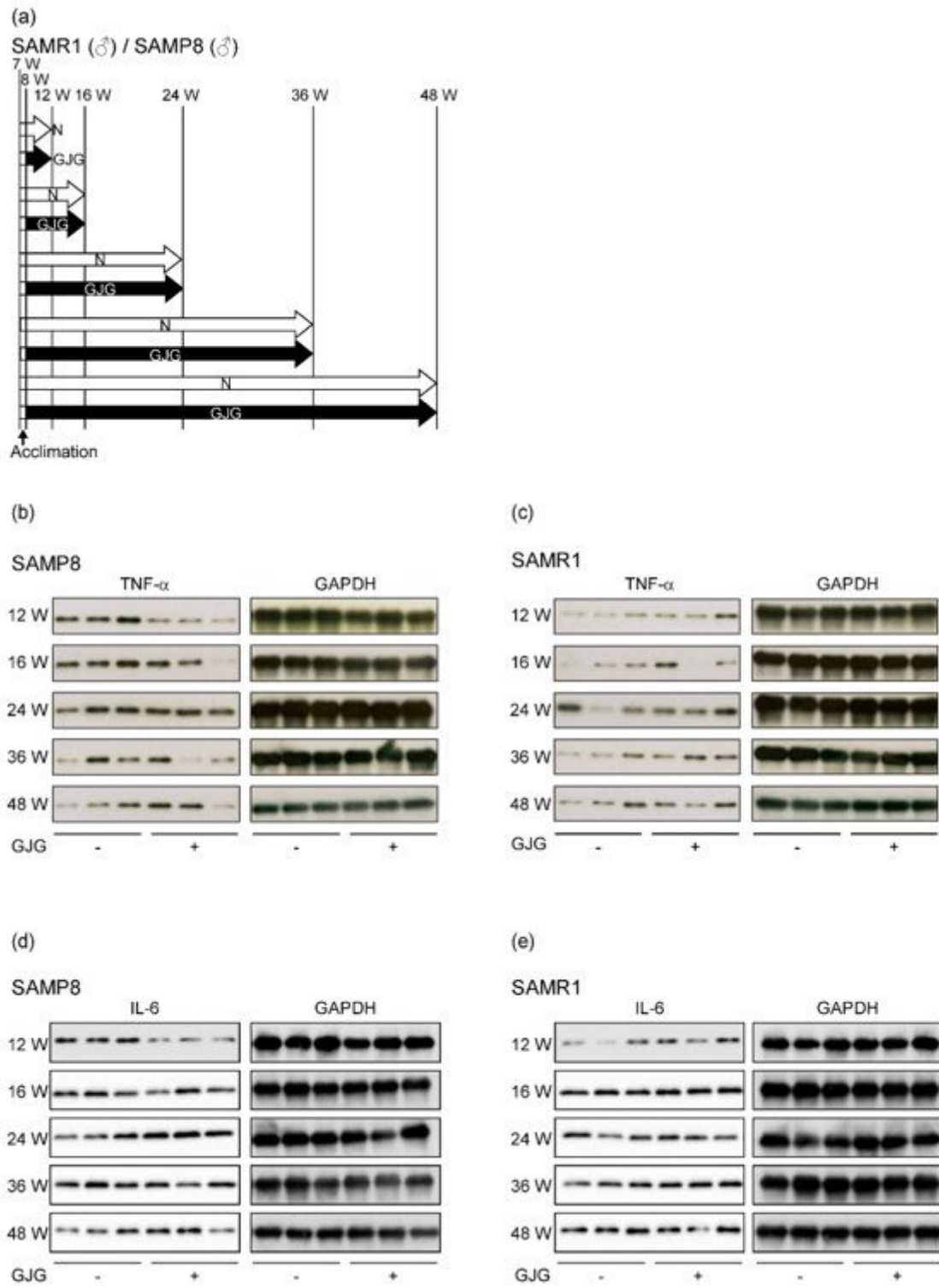
Figure 1

Suppressive effect of GJG on TNF-α production in the soleus muscle of SAMP8 mice. Experimental design of GJG administration from 12 weeks to 48 weeks in SAMP8 and SAMR1 mice (a), time course study of TNF-α expression in the soleus muscle of SAMP8 mice (b) and in the soleus muscle of SAMR1 mice (c), time course study of IL-6 expression in the soleus muscle of SAMP8 mice (d) and in the soleus

muscle of SAMR1 mice (e). The left panel shows the western blotting analysis of TNF-α from 12 weeks to 48 weeks. GAPDH is shown as a loading control.
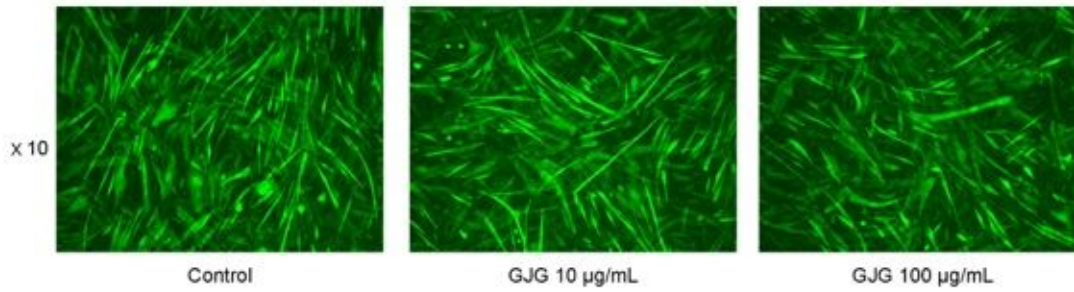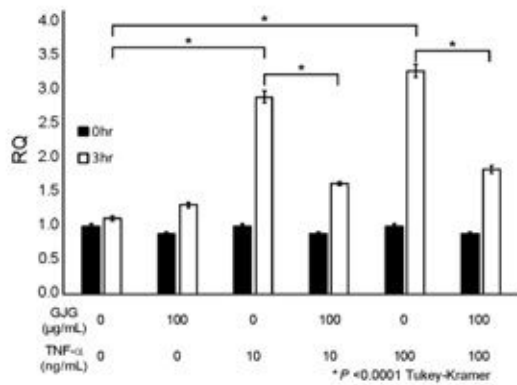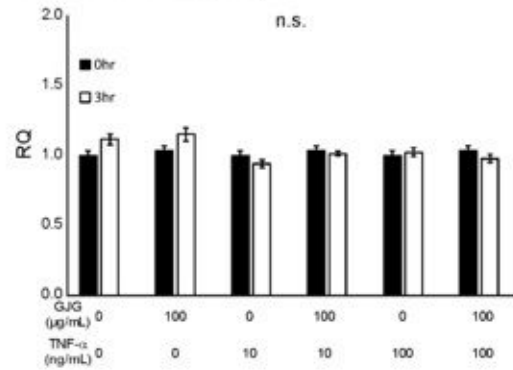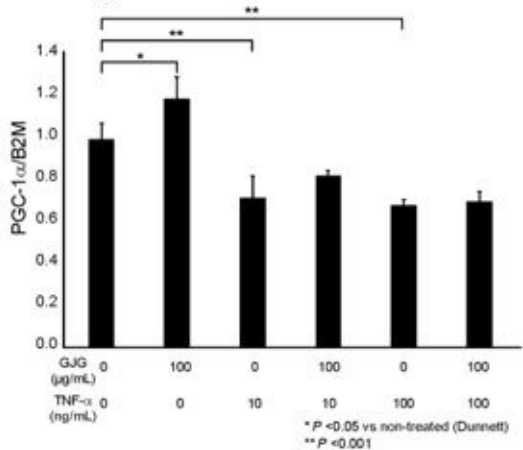
Figure 2

Effect of GJG (10-100 mg/mL) on C2C12 myotube cells with/without TNF-α (10-100 ng/mL). Immunofluorescence staining with anti-sarcomeric actinin antibody (a). The expression levels of MAFbx using a real-time PCR system (b). Data are presented as means ± SD and analyzed using the Tukey-

Kramer test (* P<0.0001 indicates a significant difference, N = 3), the expression levels of MuRF-1 using a real-time PCR system (c), the expression levels of PGC-1a using digital PCR (d). Data are presented as means ± SD and analyzed using Dunnett's test (** P<0.001, * P<0.05 indicates a significant difference vs. non-treated, n = 3).

(a)
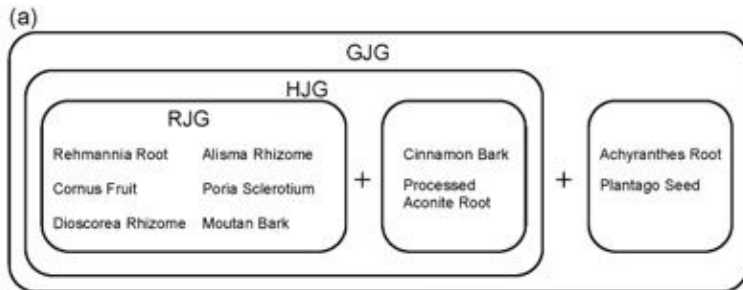
(b)

Constituent herbal medicine of GJG	Chemical compound	Inhibitory effect of production of TNF-α (%)	Cell viability (%)
Rehmannia Root	Isoacteoside	127.68	95.76
	Catalpol	102.14	71.48
	Aucubin	70.95	99.47
Cornus Fruit	morroniside	99.16	90.14
	Loganin	82.77	95.35
Alisma Rhizome	Alisol A	79.01	46.51
Moutan Bark	benzoylpaeonniflorin	113.54	99.23
	Paeoniflorin	159.12	97.30
	2'-hydroxy-4'-methyoxyacetophenone	174.57	101.10
	1,2,3,4,6-penta-O-galloyl-β-D-glucopyranose	57.86	15.42
Cinnamon Bark	cinnamaldehyde	34.52	100.17
Processed Aconite Root	Benzoylmesaconine	66.18	100.96
	Mesaconitine	77.80	99.97
	Neoline	83.64	93.06
	Benzoylhypaconine	68.19	95.08
	Benzoylaconine	89.36	98.50
Achyranthes Root	Chikusetsusaponin V	31.50	99.67
	inokosterone	65.61	100.69
Plantago Seed	Geniposidic acid	54.56	93.21
	Aucubin	70.95	99.47
Gardenia Fruit*	Genipin*	114.78	100.08

This is not a constituent herbal medicine of GJG and used as a negative control.

(c)
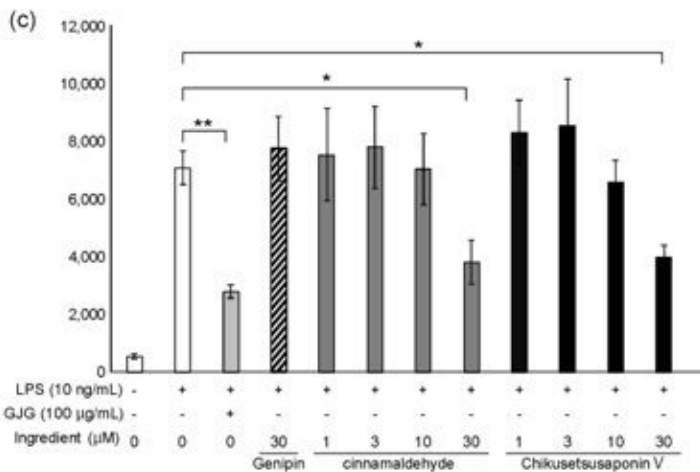
*P <0.05 vs LPS(10 ng/mL)-treated alone   **P <0.01 vs LPS(10 ng/mL)-treated alone   Tukey-Kramer

Figure 3

Inhibitory effect of cinnamaldehyde and Chikusetsusaponin V on the production of TNF-α from RAW264.7 cells stimulated with LPS. Herbal medicine composition of GJG, HJG, and RJG (a), suppression and cytotoxicity effect of chemical compounds from GJG components on the production of TNF-a from RAW 264.7 cells stimulated with LPS (b), inhibitory effect of cinnamaldehyde and Chikusetsusaponin V on the production of TNF-α using an ELISA system (c). Data are presented as means ± SD and analyzed using the Tukey-Kramer test (** $P<0.001$, * $P<0.05$ indicates significant difference vs. only LPS-treated RAW264.7 cells, n = 3).


(a)

TLR4						
MyD88						
GAPDH						
LPS (10 ng/mL)	-	-	+	+	+	+
GJG (µg/mL)	0	100	0	10	100	0
DEX (µM)	0	0	0	0	0	10

(b)

p-IκBα (Ser32)							
IκBα							Cytosol
GAPDH							
NF-κB p65							
PCNA							Nuclear
LPS (10 ng/mL)	-	-	-	+	+	+	
GJG (µg/mL)	0	10	100	0	10	100	

(c)

|								
NF-κB p65								Nuclear
PCNA								
LPS (100 ng/mL)	-	+	+	+	+	+	+	+
Chikusetsusaponin V (µM)	0	0	150	50	15	0	0	0
GJG (µg/mL)	0	0	0	0	0	0	100	0
DEX (µM)	0	0	0	0	0	0	0	100
1% FBS	-	-	-	-	-	+	-	+
1% DMSO	+	+	-	-	-	-	-	-
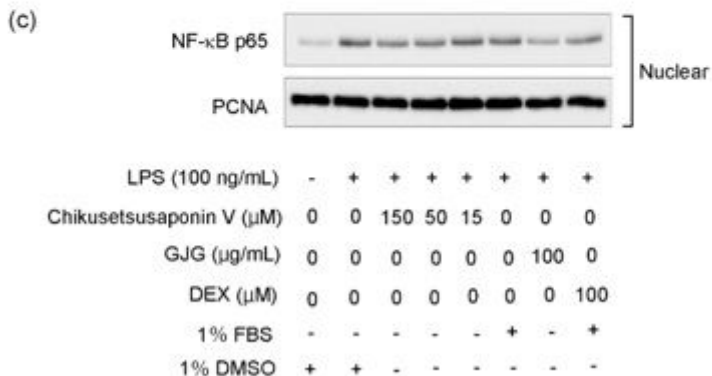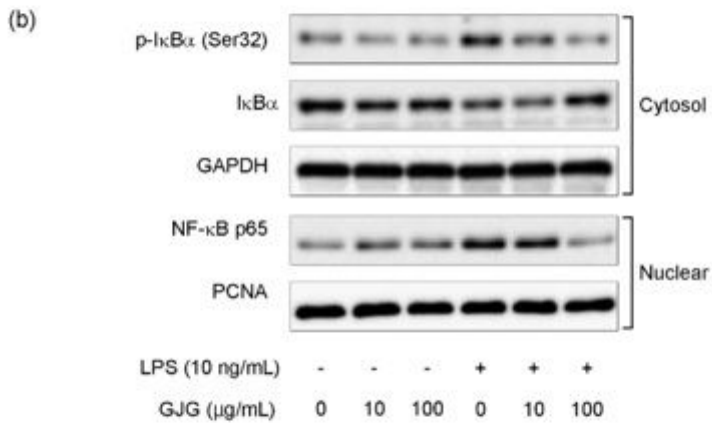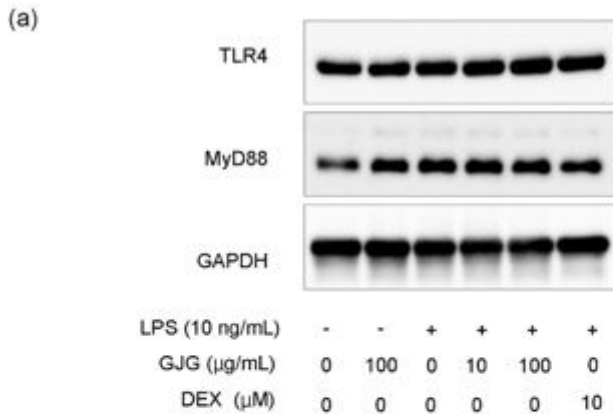
Figure 4

GJG and Chikusetsusaponin V suppress the translocation of NF-kB p65 in the RAW 264.7 cells stimulated with LPS. Western blotting analysis of TLR4 and MyD88 is shown. GAPDH is shown as a loading control (a) Western blotting analysis of IkBa and phosphor-IkBa in the cytosol and NF-kB p65 in the nuclei. GAPDH is shown as a loading control in the cytosol and PCNA in the nuclei (b) Western blotting analysis of NF-kB p65 in the nuclei. GAPDH is shown as a loading control in the cytosol and PCNA in the nuclei (c). Dex:Dexamethasone as used positive control.

(a)

Chikusetsusaponin V

(b)

(c)
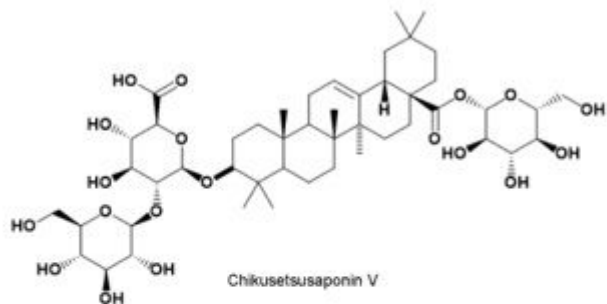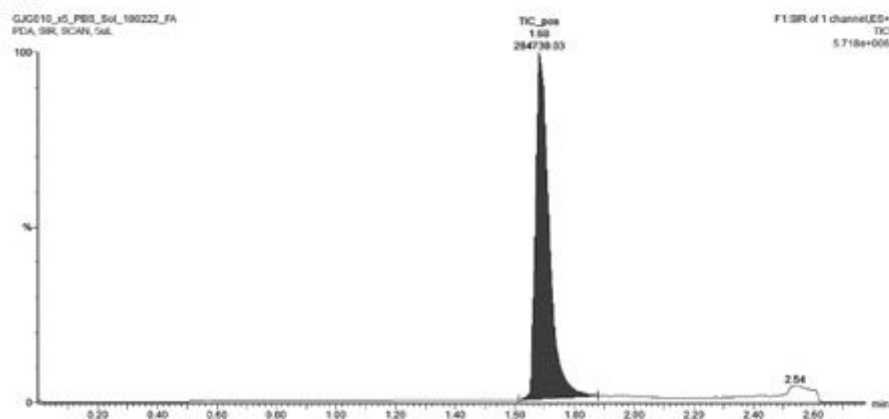
| No	Sample	Conc.(μM)	DMSO(%)	Retention Time	Area
1	Chikusetsusaponin V	500	5	1.68	286,219.938
2	Chikusetsusaponin V	50	5	1.68	31,043.129
3	Chikusetsusaponin V	500	1	1.68	284,739.031

(d)

Cpd.	Papp (cm/sec x 10^{-6})
Chikusetsusaponin V	<0.1

(e)

Cpd.	Value (%)			
	Human		Rat	
	10 min	60 min	10 min	60 min
Chikusetsusaponin V	86	89	88	92

Figure 5

Chemical characteristics of Chikusetsusaponin V. Structural formula of Chikusetsusaponin V (a) Single peak of Chikusetsusaponin V detected by the LC/MS system. Concentration of Chikusetsusaponin V calculated based on the area under the curve. (b) Chikusetsusaponin V was dissolved with PBS containing 1 or 5% DMSO. The solubility of Chikusetsusaponin V was calculated based on the area under the curve (c) Caco-2 permeability assay, the solutions on the top plate and the bottom plate were collected. The supernatant was analyzed by LC/MS and the apparent permeability coefficient (Papp) was calculated.(d) Metabolic stability assay: 500 µM Chikusetsusaponin V was mixed with liver microsomes, coenzyme group (NADPH, G-6-P) and G6PDH Mix at 37 ˚C, for 0 min, 10 min, and 60 min. The supernatant was analyzed by LC/MS, and the ratio of unchanged chemical compound at 10 min and 60 min compared to the unchanged Chikusetsusaponin V at 0 min as 100% was calculated (e)
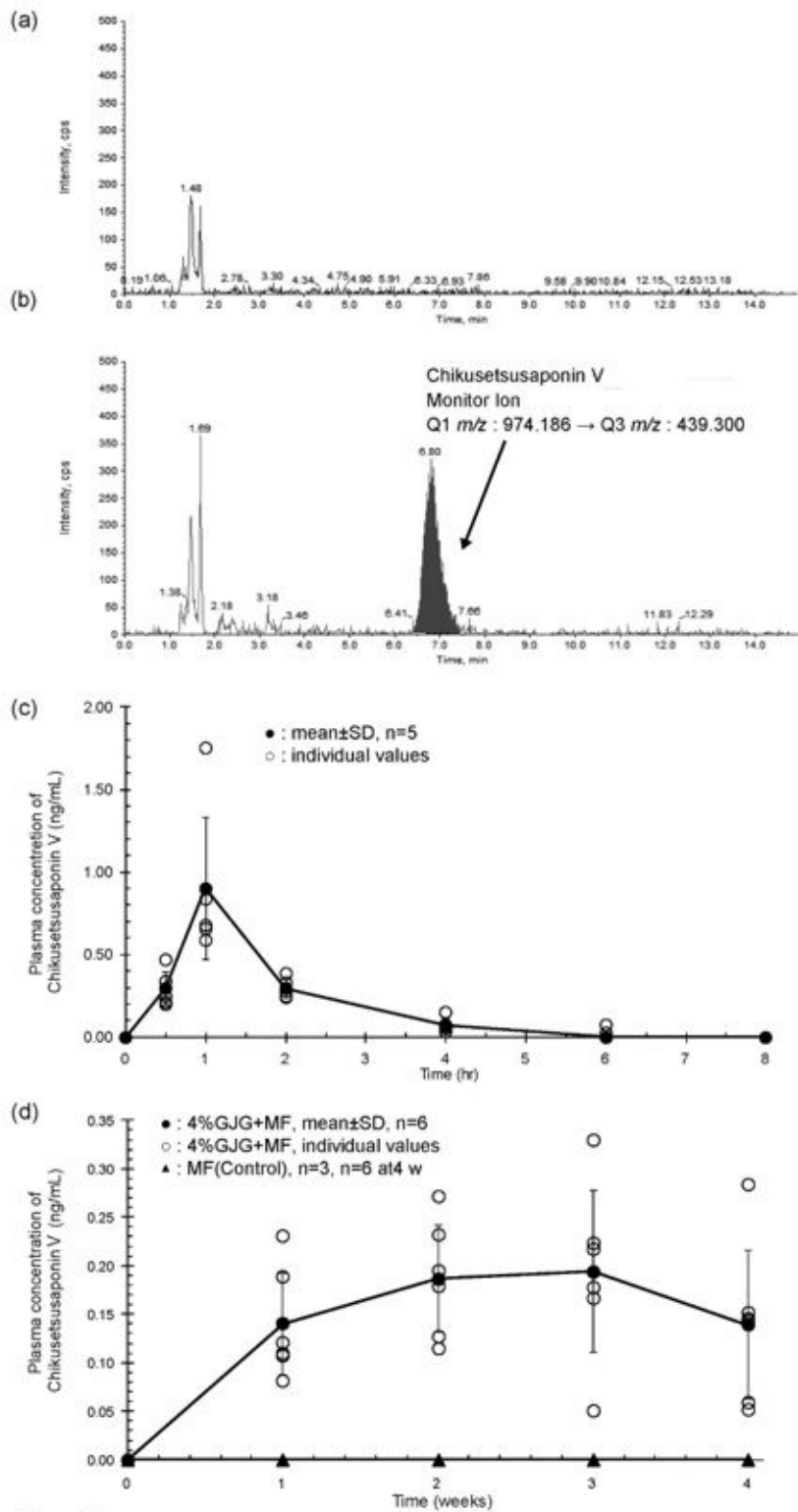
Figure 6

ChikusetsusaponinV was detected in the plasma following oral administration of GJG. No administration of GJG (a) Single peak of chikusetsusaponinV is detected in the plasma of CD1 mice (ICR) (b) After 16 h of fasting, GJG extract powder 1 g/kg was given orally to 8-week-old male CD1 (ICR) mice. Plasma samples were collected before and after administration at 0.5, 1, 2, 4, 6, 8, 10, 12, and 24 h (n = 5 at each time point) (c) Eight-week-old male SAMP8 mice were fed a normal diet (n=3 from 1 week to 3 weeks, n=6

at 4weeks) or a normal diet supplemented with 4% (w/w) GJG for four weeks (n = 6 before and at each time point). Plasma samples were collected before and after administration at 1, 2, 3, and 4 weeks. For CD1 (ICR) mice, the analysis range of the calibration curve is from 0.0200 to 10.0 ng/mL and for SAMP8 mice, and the analysis range of the calibration curve is from 0.0500 to 10.0 ng / mL.

Supplementary Files

This is a list of supplementary files associated with this preprint. Click to download.

- Supplemental.docx
- Supplemental2.docx